A Review of Roughness-Induced Nosetip Transition

R.G. Batt
TRW STG, Redondo Beach, California
and
H.H. Legner
Physical Sciences, Inc., Woburn, Massachusetts

I. Introduction

THE re-entry physics community has for many years recognized the crucial role that nosetip transition plays in re-entry vehicle performance. The onset and progression of the transition front are governed by complex fluid mechanical processes that depend critically on surface roughness, wall temperature, nose-tip geometry, angle of attack, and freestream conditions. The flight analyst must make preflight predictions and postflight data comparisons incorporating a suitable transition model in shape-change code computations. Such calculations of vehicle drag and surface recession contours are sensitive to both the transition correlation and the surface roughness. This sensitivity of nosetip shape change is dramatic, as witnessed by calculated results[1,2] that show that moderate changes in either the surface roughness height (keeping the correlation fixed) or the transition correlation slope (keeping the roughness fixed) lead to markedly different transition-onset altitudes and nosetip shapes. These vehicle shape-change effects, which are in direct response to the transition process, are further compounded by the inherent stochastic behavior of boundary-layer transition and the random nature of nosetip-surface roughness. Resulting transition front asymmetries can promote asymmetric nosetip shapes that cause substantial vehicle trim dispersions.

The importance of the two key aspects of nosetip transition, i.e., the transition correlation model and the roughness character, has, of course, been pointed out by previous investigators. Although individual experiments or analyses have been self-contained and have adequately described most of the observed behavior, there still exists in the literature a lack of consistency among the various studies with regard to 1) roughness height definition, 2) transition point identification, and 3) validity and/or interpretation of specific experimental transition data. These deficiencies have limited the extent to which previous studies can be applied and have provided the primary motivation for the present investigation.

The current paper, which essentially summarizes results obtained from the detailed study reported in Ref. 2, reviews previous research on nosetip transition, re-examines surface roughness characterization, and describes a nosetip correlation model based in part on the critical Reynolds number approach as well as on a re-evaluation of experimental data. In the sections that follow, the emphasis will be upon the consistent evaluation and detailed review of the *ground-test data* on nosetip transition. A common roughness height definition is developed and subsequently used to re-analyze the data base for wind tunnel, ballistic range, and free-flight experiments.

II. Review of Previous Studies

Excellent reviews of re-entry vehicle nosetip transition have been published by many investigators.[3-6] These workers have discussed the basic issues involved in the onset and progression of nosetip transition and have described the shape-change-sensitivity issues identified in the Introduction. Two recent papers[7,8] provide an in-depth review of roughness-dominated nosetip transition and serve as a good introduction to the present study.

When this study was initiated, the ballistic range transition data of Reda[5] were just becoming available and the Demetriades nozzle wall experiments[7] had just been completed. The only extensive source of roughness-induced transition data previously available was the Passive Nosetip Technology (PANT) program undertaken at Aerotherm.[10,11] Together, these three sources of ground-test data have provided essential background details contributing to our current understanding of the nosetip transition problem.

Richard G. Batt is a member of the Engineering Staff of the Engineering Sciences Laboratory at TRW. He received his Bachelor of Aeronautical Engineering degree from Princeton University and his M.S.E. and Ph.D. (1967) from the California Institute of Technology. Dr. Batt has conducted experimental research in the fields of turbulent chemical kinetics, shear-flow turbulence, hypersonic wakes, blast wave phenomenology, and wind tunnel studies of missile aerodynamics. In most of these investigations, Dr. Batt has applied the methods of hot-wire anemometry to determine detailed results for the mean and turbulent structure of the local flow. He is a Member of the AIAA and is the author or coauthor of over 15 technical publications.

Hartmut H. Legner is a Principal Scientist at Physical Sciences, Inc. He received his B.S. (aeronautical engineering) and M.S. (astronautics) from the Polytechnic Institute of Brooklyn and his Ph.D. from Stanford University in 1971. Dr. Legner has performed research in fundamental shear-flow turbulence, stability of jets and wakes, and basic boundary-layer theory. He has also contributed to various laser-related fluid dynamic research projects including the design of high-energy cw subsonic CO_2 lasers, laser propulsion, acoustic suppression in laser cavities, and laser aerodynamic windows. Most of these studies were carried out while Dr. Legner was with the Avco-Everett Research Laboratory and with TRW's Engineering Sciences Laboratory. At the present time, he is specializing in shock-wave/boundary-layer interaction studies and in boundary-layer transition phenomena. He is a Member of the AIAA as well as several honor societies: Sigma Gamma Tau, Tau Beta Pi, and Sigma Xi.

Presented as Paper 81-1223 at the AIAA 14th Fluid and Plasma Dynamics Conference, Palo Alto, Calif., June 23-25, 1981; submitted July 20, 1981; revision received March 25, 1982.

The PANT program was carried out in the early 1970's and included both analytical and experimental work in roughness-dominated nosetip transition. The experimental results[9-11] were correlated by the now famous PANT transition onset correlation

$$Re_{\theta T} = 215\,\psi^n,\ n = -0.7 \tag{1}$$

where $\psi \equiv (k/\theta)T_e/T_w$ is the disturbance parameter characterizing the surface roughness k. The wind-tunnel transition experiments were conducted over a large range in ψ ($\approx 10^{-2}$ - 10) and roughness [$k \approx$ .015-1.02 mm (0.6-4.0 mil)].

Although most of the PANT data have been used extensively without question, two difficulties with the data base are evident at low roughness values. These difficulties arise due to the unavoidable and familiar issue of performing wind-tunnel transition experiments with smooth and/or "small" surface roughness models wherein freestream disturbances become a factor in the transition process. For example, transition data from the PANT smooth model tests, which corresponded to $Re_{\theta T}$ values $\simeq$100-200, were found to be influenced by the effects of freestream disturbances,[10] and thus the published PANT data base does not include these data. Interestingly enough, PANT's "small" roughness experiments [$k \simeq$ .015 mm, (0.6 mil)] "measured" comparable $Re_{\theta T}$ results. It follows therefore that these .015-mm (0.6-mil) data are most probably influenced by tunnel disturbance phenomena and should therefore similarly not be included in summarized transition results. Note that the slope n of the PANT correlation curve ($= -0.7$) is dependent to a great extent on these low k/θ results, which unfavorably bias the current PANT transition correlation through use of "low-signal-to-noise" data. A substantially steeper slope n is suggested, for example, when the .015-mm (0.6-mil) PANT results are excluded from the data base.

In addition to this PANT data limitation at low k/θ, the basic question of the appropriate correlation model to use under the smooth-wall limit condition is also still unresolved. For example, some flight data indicate that Re_θ values as high as 500-600 were experienced without the nosetip undergoing transition. PANT and the Nosetip Transition Experimentation Program (NTEP)[12] results, on the other hand, suggest an upper limit for $Re_{\theta T}$ of only 150-300. This issue is significant since the domain where constant-slope data "knee over" and fair into the smooth-wall or maximum $Re_{\theta T}$ limit coincides with conditions typical for the onset of re-entry nosetip transition ($\psi \approx 1$). The more recent Demetriades experiments[7] on the nozzle wall indicate a smooth-wall $Re_\theta \simeq 500$.

Until the ballistic range data of Reda were published,[5] investigators of nosetip transition depended almost entirely on the PANT results as their main source of data on roughness-induced nosetip transition. For this reason, Reda's *independent* experiments on this problem area using the ballistic range test facility represent an important contribution. This basic set of transition measurements is significant not only because of its independent nature and range of test conditions, but also because it provides unique results on the performance of real-material nosetips.

Reda's results are divided basically into two parts. One part describes the details and results of his experimental program, and the other assesses the range data in relation to previous correlation studies. This assessment may have been limited, however, through use of curve fits to the PANT data [including the .015-mm (0.6-mil) results] rather than actual data points. Also, the favorable comparison[8] of the range data with the Dirling et al.[4] correlation may be more apparent than real since the range data were presented without curvature correction whereas the Dirling results included this correction term. Purported ablation during the flight down the range is given as the reason for permitting such a data comparison approach. A further difficulty, and one also raised by Reda himself, is the definition of the appropriate surface roughness inducing transition for the preablated carbon-carbon models.

How do the ballistic range data compare with the PANT data base? A direct comparison in PANT coordinates ($Re_{\theta T}$-ψ) between ballistic range data on nosetip transition for graphitic and carbon-carbon nosetips[5,13,14] reveals[8] noticeable discrepancies with the PANT *transition correlation model.*[15] In some cases, transition Reynolds numbers $Re_{\theta T}$ from the ballistic range experiments are even lower than PANT values. This result is surprising since ballistic range transition data should not suffer from freestream disturbances occurring in wind tunnels. This lack of validation of the PANT data correlation under higher Mach number, higher Reynolds numbers, and realistic surface roughness conditions was a disturbing result. Either one facility or data set was providing misleading results or the present scaling variables were improperly selected. This disparity between range and tunnel data is addressed subsequently in the current review.

The third important set of ground-test results on nosetip transition is the nozzle wall study by Demetriades.[9] Measured results obtained from this investigation are well documented and cover a wide range of disturbance parameters extending from the smooth-wall ($\psi \simeq 0.3$) to the rough-wall ($\psi \simeq 3$) domain.

In analyzing his experimental results, Demetriades finds that the measured data agree well with blunt-body experimental results. In addition, he concluded[7] that his data and those of Laderman[16] appear consistent with PANT onset data correlation when the correlation is extrapolated an order of magnitude lower in the disturbance parameter ψ than achieved experimentally. The agreement between experiments as suggested[7] is, however, *not* realized if a common roughness height definition is used in the data comparison. For example, the nozzle wall data as documented by Demetriades are based on average-peak-to-average-valley (APV) differential, which is *not* the same definition as used in the PANT correlation model, i.e., significant peak-to-valley (SPV) differential. In fact, when characteristic roughness heights for these two approaches are compared, it is found[2] that the nozzle wall surface roughness based on the SPV method is 2.3 to 3 times larger, in general, than the corresponding roughness values determined by the APV approach. Interestingly enough, by "adjusting" Demetriades' data using SPV roughnesses, it is found that the data base shifts to larger ψ values and results in transition data that fair satisfactorily into the *ballistic range* measurements.

Three sources of experimental nosetip transition data have been emphasized up to this point. There are, of course, many other investigations, dating back to the 1950's when transition data appropriate to rough blunt-body geometries were first obtained. The results of these specific studies are also incorporated into the present study and are referenced appropriately.

In several of the correlation models (e.g., PANT), the disturbance parameter ψ is linearly related to k [c.f., Eq. (1)]. In this form the surface roughness is characterized by a *single* roughness height k, even though surface roughness for typical ablated nosetips exhibit spatially random or statistically distributed behavior in terms of roughness height as well as disturbance spacing and shape. As noted above, all PANT data are correlated in terms of significant peak-to-valley roughness heights, whereas other ground-test experiments have used such height definitions as rms (both overall and element height only); average, mean, 20th percentile, inferred (flight *and* arcjet), microroughness (laminar/turbulent, composite, z yarn, etc.), shape sensitive, average-peak-to-average-valley differential, and even "effective" sand-grain roughness height. This use by investigators of an arbitrary and/or inconsistent roughness characterization definition is misleading and makes difficult the work of the flight dynamicist who attempts to predict nosetip transition, but is not given a *consistent* definition for surface roughness height.

Some investigators have even back-calculated an "inferred" roughness based upon matching an experimental observation, e.g., vehicle drag. All of these roughness height definitions are attempts by the investigator to identify the height promoting transition.

For sand-grain roughnesses, typical of graphite nosetips in a laminar heating environment, it has been found that inferred values for k compare favorably with mean or 50th percentile roughness heights as *measured* from posttest specimens. Conversely, inferred roughnesses for carbon-carbon weave materials, such as 223, are orders of magnitude smaller than measured macroroughness values. In fact, inferred k's are more comparable to *microroughness* levels corresponding to the ends of protruding fiber bundles. This inconsistency between inferred and measured roughness disturbance heights is further complicated by the fact that wind-tunnel testing of carbon-carbon simulation models has not yet been undertaken. Thus the PANT-based transition correlation model represents a bias toward sand-grain or brazed-particle types of roughness. The inclusion of ballistic-range carbon-carbon transition measurements into the present data base helps to generalize the correlation model.

The experimental research on nosetip transition has, in general, been quite successful in helping to clarify the physics of the problem. In contrast to these efforts, theoretical treatments of nosetip transition have been relatively limited in success. The reason for this is the necessity of including the surface roughness as an essential parameter in the analytical model. Anderson[17] has previously evaluated three theoretical methods for the prediction of nosetip boundary-layer transition. Two of the three methods[18,19] sought to use a turbulence model to predict transition for both smooth- and rough-wall circumstances. The other model attempted to predict transition using the more traditional linear stability theory.[20]

The two models that approach the transition question from the turbulence perspective argue that the turbulence model should become increasingly valid as turbulence intensities build up, especially if the correct low (turbulence) Reynolds number terms are contained in the model. The stability theory approaches the transition problem from the small-perturbation point of view. It is certainly true that transition is the result of the laminar boundary-layer flow becoming unstable; however, the Merkle et al. approach[21] considers only growth of the initial (linearly unstable) perturbation. It has not been established from first principles how this linear perturbation proceeds to grow and eventually causes the laminar layer to behave in a turbulent manner. The "e^9" factor is empirical. What is the corresponding growth factor for nosetip transition?

Both types of analyses described here are valid over only part of the flowfield. Neither approach can be extended over the entire range from laminar instability to developed turbulence; however, Wilcox and Chambers[18] made an attempt to bridge this gap for incompressible flat-plate boundary-layer transition, with some success. Further work could be carried out using nonlinear stability theory together with an accurate low Reynolds number turbulence model. Unfortunately, such an ambitious model has not even been structured for the *smooth*-wall, incompressible, flat-plate case, let alone for nosetip transition with effects of compressibility, spherical nose geometry, and, importantly, surface roughness. Therefore, it would appear that the theoretical analysis of real nosetip transition is in a state of only "initial" development. Re-entry vehicle designers must therefore utilize the results of the many correlation studies[6,22] that have endeavored to make several sets of experiments obey universal laws.

III. Roughness Characterization

The surface roughness on a vehicle nosetip is typically characterized by a single quantity: the roughness height k. The definition of the roughness height—or more specifically the "roughness" height that induces boundary-layer transition—is difficult to identify. Roughness elements characterized by k also have a width b and an element spacing l. In most cases the surface texture is rather complex, with various (random) values of k, b, and l characterizing the surface. A subset of this general situation has been identified for woven carbon-carbon re-entry vehicle heat shields, where the roughness has a bimodal character. One can identify microroughness and macroroughness elements in these materials. At issue for re-entry nosetip transition is the manner in which the presence of micro/macroroughness affects transition and whether or not a suitable averaged single intermediate value of roughness is appropriate for analysis.

At the outset of the present study, it was realized that an important consideration in nosetip transition was the issue of surface roughness characterization. In some cases correlation models were compared to and/or based on measured roughness data corresponding to different definitions of surface roughness. Most investigators recognized this issue,[5,9,10,13,14] and in many cases qualified their findings, but, because of inherent technical features and/or limitations to their experimental approach, they were led, in their data correlation analysis, to select a roughness height designation not necessarily consistent with that used by other workers.

A. Surface Roughness Measurement

Typically either one or both of two methods have been used to measure surface roughness. These are surface profilometer measurements and detailed processing of optical/photomicrograph data ($\sim 350\times$) from sectioned-nosetip models. In the first method, an automatic recording profilometer system is set up with a sharp-point stylus and the data are analyzed by a computer program to provide rms roughness, amplitude probability densities, element height distributions, as well as other basic statistical properties. A representative profilometer trace[23] is given in Fig. 1a for PANT's 1.6-mil (.041-mm) roughness model. The quantities in this figure are identified below. For the moment, consider the profilometer trace as a sample of the surface profile in a single plane cutting the model.

In the photomicrograph method of surface roughness characterization, the roughened specimen is sectioned, vaccum mounted in room-temperature setting plastic for maximum edge retention, and then polished on its sectioned face to highlight surface roughness elements. Microscopic measurements of surface roughness are then made with a calibrated eyepiece to determine element height, spacing, and width. These measurements make use of an optically defined apparent or reference surface.[24] Results are typically presented in the form of roughness height distributions (probability of exceedance) and in a tabular listing of statistical data. Roughness element height distributions[5] from photomicrographs are presented in Fig. 2 for real-material surface roughnesses. Shown also in Figs. 1b and 1c are the height distribution results derived from profilometer data (Fig. 1a). Unfortunately, for some of the transition data to be discussed in Sec. IV detailed roughness measurement results were not available. For example, several investigators[25-28] published only rms profilometer data, whereas others documented either profilometer results or photomicrograph data but rarely both.

In addition to element shape, investigators have also examined the effects of element spacing on transition. Intuitively, it is well accepted that for two surfaces with the same surface roughness heights the surface with larger element spacing should be expected to be relatively "smoother" in terms of transition sensitivity. Although Schlichting (Brick[29]) and Dirling[30] examined this question in terms of heat-transfer augmentation and developed a correlation to approximate the equivalent sand-grain

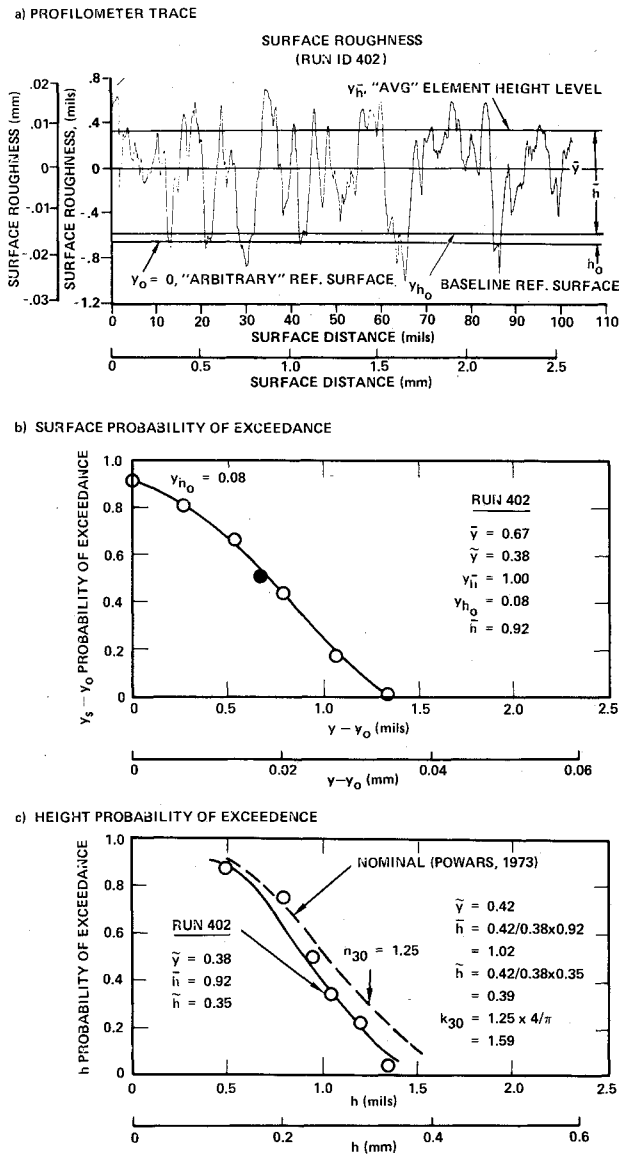

Fig. 1 Surface roughness characterization—PANT Series A ($k = 1.6$ mil, 0.041 mm; Ref. 23).

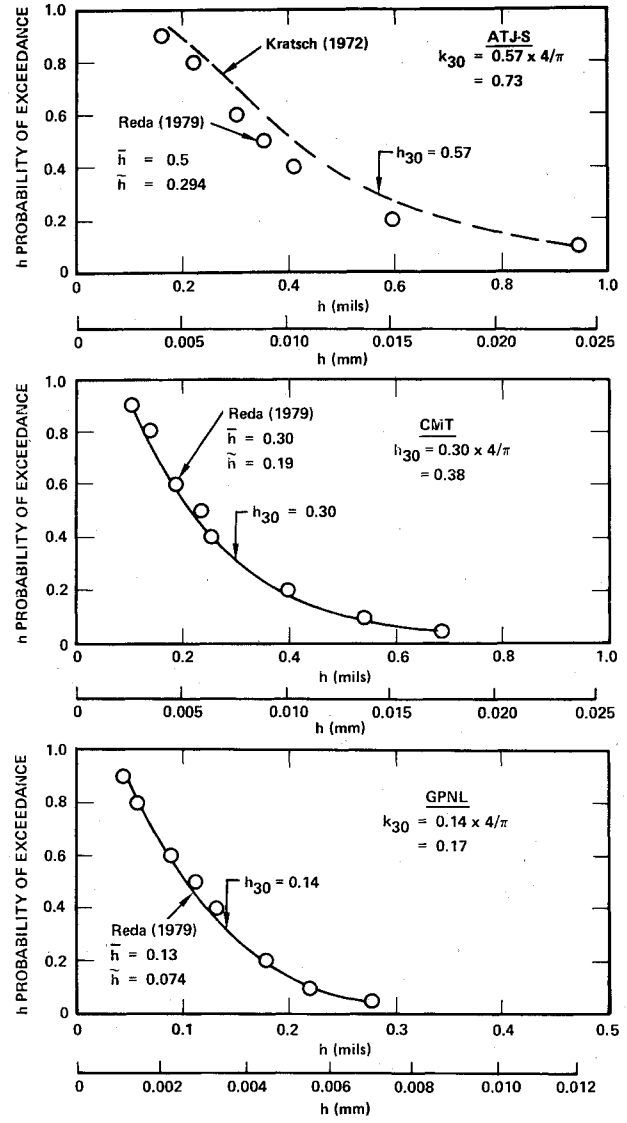

Fig. 2 Surface roughness characterization (graphite nosetip materials; Reda, 1979).

roughness as a function of element *shape* and *spacing*, no such result is available for rough-wall transition. Instead, the assumption is made that transition is dominated by the larger roughness elements, is relatively insensitive to their spacing, and can be approximately accounted for by a single parameter representation. Such an approximation may be appropriate in cases where sand-grain or random surface roughness characteristics prevail, but there exist several data sets that illustrate that element spacing[31] and shape effects such as weave orientation on carbon-carbon materials can lead to preferential transition along geometric-orientation rays.

B. "Characteristic" Roughness Height Definition and k_{30}

In this section a quantitative technique using statistical surface data will be described for determining a material's characteristic roughness height, for use in analyzing nosetip transition data. The suggested method represents an attempt to standardize the technique for measuring a nosetip's surface roughness and is based on a 30% exceedance height definition (k_{30}).

We begin the outline with a basic description of the determination of the roughness height and illustrate some of the points with the help of Fig. 1a. The experimenter who has obtained such a distribution from *any* measurement technique must perform three operations or steps in order to determine the roughness of the surface:

1) Determine the baseline reference surface (y_{h_o}) from which the individual roughness height elements can be measured.

2) Determine the probability-of-exceedance curve for the individual heights identifiable (e.g., h_i, $i = 1 - n$).

3) Determine (or select) the probability-of-exceedance value most likely to promote transition and convert the indicated height h_{PE} to k_{PE} by using the shape factor F (identified below).

Step 1

The baseline reference surface (y_{j_o}) is obtained from the entire *surface* distribution by formation of the quantity $y_s - y_o$, where y_o is an arbitrary reference surface. This surface y_o is typically chosen to be representative of the "valley" locations. Even if y_o is chosen to be many roughness heights below (above) the apparent surface, the statistics will regard the distances below (above) y_{h_o} as uniform and subtract (add) the effect. Consequently, y_o is indeed arbitrary. The abscissa x is next finely divided such that the surface is well characterized. The specific values of $y_s - y_o$ are then arranged into different bins according to their magnitude; a probability-of-exceedance curve is constructed using a finite number of bins (10-20 are usually sufficient). A typical result is shown in Fig.

1b. The open circles are the probability-of-exceedance values for the chosen bin (or range). The solid circle is the mean value $\bar{y}$ of $y_s - y_o$; it may or may not coincide with the median value $(y_s - y_o)_{PE=50}$. The solid line is a curve representation of the data points. In general, as $y_s - y_o$ gets smaller, fewer and fewer points will contribute to the probability of exceedance and the data will roll over. Since many of these values are not significant statistically, a dashed line has been extended from the bulk of the distribution toward the 100% probability-of-exceedance value. This intercept value is y_{h_o}, and it identifies the baseline reference level. A more specific means of determining y_{h_o} would be to fit the data between a probability of 20 and 80% using a straight line and then extend it toward the 100% value. Note that the concept of a baseline reference surface has been in use for some time by workers characterizing a material's surface roughness. The main distinction, however, between the present approach in selecting the location for this surface and previous methods is that prior techniques were based on an arbitrary and/or "optically apparent" surface, whereas the present technique corresponds to a *quantitative* definition that is relatively independent of experimental bias.

Step 2

The roughness height probability-of-exceedance curve can now be determined by measuring individual peaks from the baseline reference line y_{h_o}. A *height* distribution curve (where h is defined as measured from y_{h_o}) is shown in Fig. 1c. The h distribution as defined has a value at 100% as well as 0%. Between these values, there is typically a Gaussian profile, as shown by the data points and the faired curve. Figure 1c is the critically important statistical representation of the roughness height h on the surface of interest.

Step 3

Two more judgments must be made before the roughness of the surface can be defined. First, the h probability-of-exceedance value most likely to promote transition must be selected. The height h_{PE} corresponding to this probability is then taken from a curve such as Fig. 1c. Second, h_{PE} must be modified according to the shape factor F.

As discussed by Dirling,[32] measurement of roughness elements by any of the techniques described will result in measured heights h_{PE} smaller than true element heights k_{PE} because the plane of measurement does not pass through the peak of *each* roughness element. To correct, for this shape effect, the measured h values are increased by a geometric factor, i.e., $k_{PE} = Fh_{PE}$ $(F \geq 1)$. The quantity F is simply the probability of cutting through any height of a specific element shape; in other words, one averages over the element shape curve. Several examples are given by Dirling.[30] By far the most common assumption used by investigators is the hemispherical one $(4/\pi)$—roughened graphitic materials appear to correspond to such a shape. As noted by Dirling,[30] F is in the range of 1 to 2 for realistic roughness elements.

To illustrate the present surface characterization approach, consider again the PANT profilometer data for a .041-mm (1.6-mil) surface roughness sample (specimen 402), as given in Fig. 1. This figure not only indicates the technique described here for defining the baseline reference surface, but also illustrates the steps necessary to convert profilometer data to height probability-of-exceedance results (Fig. 1c). The data as plotted do not correspond exactly to the *nominal* model roughness, as can be seen by the fact that overall rms roughness $\bar{y}$ for the data of Fig. 1 was .010 mm (0.38 mil) for the noted specimen (402) as compared with specified nominal values of .011 mm (0.42 mil).[10] Shown also in Fig. 1 are Gaussian distributions corresponding to the average and standard deviation height data for both the surface roughness as measured herein and the estimated nominal roughnesses (dashed line). This latter result, which approximates the probability-of-exceedance distribution for the nominal .041-mm (1.6-mil) data, was determined by adjusting the mean $(\bar{h})$ and rms $(\tilde{h})$ data by the $\bar{y}$ ratio between the documented profilometer results and the published *nominal* data.

The purpose behind developing probability-of-exceedance distributions for the PANT data base is to determine, at least approximately, which percentile height corresponds to PANT's significant peak-to-valley height. This latter roughness height definition is described[23] as the "distance between significant peaks and the significant valleys, but is not the distance from the very highest peak to the lowest valley." Most transition investigators have recognized that the "larger" roughness elements are primarily responsible for triggering transition, as in fact discussed by Reda and Leverance[33] and Bishop,[34] who suggested the 20th percentile element height as a probable candidate. Figure 1 illustrates that, *to be consistent with PANT's height designation, an element height corresponding approximately to the 30% distribution value provides favorable comparison with significant peak-to-valley heights when allowance is made for shape effects.* Because of the wealth of data generated during the PANT program, all transition data reviewed herein have therefore been processed and reduced in terms of 30% exceedance heights (k_{30}) in order to provide a consistent and practical comparison with the PANT data base. The NTEP roughness data exhibited substantial differences between author-quoted roughness heights (based on APV differential) and 30th percentile values derived from published profilometer plots (Table 1). It is interesting to note that the graphite roughness data for Reda's ballistic range experiments agree favorably with the present 30% distribution heights (Fig. 2). This latter favorable comparison is not evident when examining the Reda roughness heights for his carbon-carbon weave models, as is illustrated in Fig. 3. This difference is believed due to flight environment effects, as discussed in Sec. IV.

C. Roughness Data

The characteristic surface roughness data for the nosetip experiments on rough-wall transition that were reviewed during the current study are summarized in Table 1. Where available, author-suggested data are included as well as direct

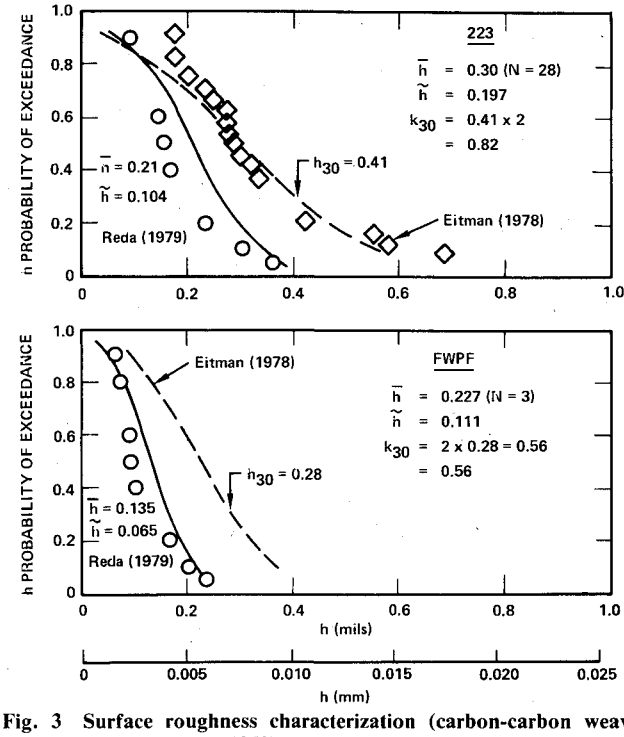

Fig. 3 Surface roughness characterization (carbon-carbon weave nosetip materials; Reda, 1979).

Table 1 Roughness height characterization summary, mm

REF	K_{TYPE}	Y_{RMS}	K_{REF}	H_{AVG}	H_{50}	H_{30}	K_{30} (B)
9,	1.6-G	-	40.6	-	25.4	31.8	40.6
10,	3.0-G	-	76.2	-	-	-	76.2
11,	3.0-B	-	76.2	-	-	-	76.2
38,	10.0-B	-	254.	-	-	-	254.
41	40.0-B	-	1016.	-	-	-	1016.
↓	3.5-G	-	88.9	-	66.0	70.0	88.9
51	3	-	76.2	-	-	-	76.2
31	4	-	101.6	-	-	-	203.2
↓	25	-	635.	-	-	-	635.
↓	50	-	1270.	-	-	-	1270.
25	.4	2.54	-	-	-	-	10.2
↓	.8	5.08	-	-	-	-	20.3
26	.025	.635	-	-	-	-	2.5
27	.025	.635	-	-	-	-	2.5
28	.0025	.064	-	-	-	-	.25
52	4	-	101.6	-	-	-	101.6
12,	IIA	-	50.8	-	61.0	101.6	129.5
44	IIB	61.0	121.2	-	88.9	116.8	152.4
↓	IVA	33.0	59.9	-	53.3	66.0	83.8
↓	IVB	-	43.2	-	-	-	43.2
7	400	6.6	7.9	15.0	-	18.5	12.6
↓	320	13.2	20.1	31.0	-	38.1	48.5
↓	280	13.7	22.6	34.0	-	41.4	52.8
↓	220	24.9	38.4	55.9	-	69.3	88.4
↓	120	37.6	47.8	86.4	-	106.7	135.9
↓	100	57.4	85.9	126.7	-	157.5	200.4
↓	80	70.1	112.5	169.2	-	206.8	263.1
↓	60	73.4	100.6	159.5	-	198.9	253.2
5,	ATJ-S	7.4A	16.3	12.7	10.4	14.5	18.5
8,	CMT	4.8A	9.7	7.6	6.1	8.1	9.6
33	GPNL	1.8A	4.3	3.3	3.0	3.6	4.3
↓	223	2.5A	21.3	5.3	4.1	5.1	20.8C
↓	FWPF	1.8A	14.2	3.6	2.5	4.3	14.2C
14	ATJ-S	-	14.0	10.9	8.9	12.7	16.3
↓	994-PR	3.30	7.6	-	-	-	13.2
↓	994-PA	-	14.5	11.4	9.4	11.4	11.5
↓	WPR-FT	3.56	10.2	-	-	-	14.2
↓	WPR-TK	-	7.4	5.8	5.3	6.4	8.
↓	223	-	6.4	5.1	4.6	7.4	9.9D
2	ATJ-S	7.4A	-	10.9	10.4	14.5	18.5
↓	223	5.1A	-	7.6	7.6	10.4	20.8D
↓	FWPF	3.0A	-	5.8	5.8	7.1	14.2D

A H_{RMS}
B $K/H = 4/\pi$ EXCEPT WHERE NOTED
C $K/H = 4$
D $K/H = 2$

(profilometer/photomicrograph) and inferred (arcjet) element height values. Root mean square profilometer results correspond to *surface* standard deviation data, whereas mean and rms data from photomicrograph measurements represent *element height* results. The average and mean heights as noted are with reference to an optical reference surface and correspond to the statistical average and the 50th percentile exceedance value, respectively. The data also include the shape effect correction F discussed previously and the recent results of Demetriades[9] based on APV differential. The *inferred* roughness heights were derived from the PANT correlation model using known freestream flow conditions, calculated boundary-layer properties, and shape-change dependence on transition onset (arcjet testing).

As can be seen by a review of Table 1, there exist for a given model substantial differences in roughness height values depending on which definition is used. One approach to establishing the correspondence between roughness height definitions was put forward in the early days of the PANT program[10,23] when profilometer rms measurements were found to compare favorably with a linear approximation to PANT's significant peak-to-valley designation. By showing that the rms surface roughness data correspond to approximately 25% of SPV roughness, those earlier results for which investigators quoted only rms roughness could then be related to the PANT data base in a consistent, although approximate manner. In a similar manner, the k_{30} height definition serves to provide investigators with a practical and consistent method for characterizing a material's surface roughness. Unfortunately some published transition data have been limited by the unavailability of detailed and documented roughness measurements. In some cases the roughness data have been measured but results have not been published, thus making necessary an approximate treatment of certain results.

IV. Ground-Test Data on Nosetip Transition

Important nosetip transition data have been obtained over the years in many different test facilities. These include high-enthalpy arcjets, free-flight rocket tests, conventional wind tunnels, and ballistic range facilities (Table 2). The complex nature of re-entry vehicle nosetip transition necessitates testing in this manner in order to obtain complementary results, since no one facility completely simulates all aspects of nosetip transition.[35] The Reynolds number capability of hypersonic wind tunnel facilities[35] ($M>10$) is an order of magnitude less than that experienced by a typical re-entry vehicle. On the other hand, although performance in a ballistic range provides a closer simulation of Reynolds and Mach numbers, some test limitations arise because of short test times, limited wall temperature range, and restrictions on type and amount of flowfield measurements. Similar comments are appropriate for arcjet testing, which provides still another method for matching stagnation pressures and enthalpies during atmospheric re-entry. Typical experimental capabilities are given in Table 2. Since the complete simulation of such re-entry conditions as Mach number, Reynolds number, and total enthalpy is still beyond the state-of-the-art, ground-test experiments have been conducted to complement and extend results from other facilities and thereby approximate the conditions of the full-scale problem.

In presenting transition results from the many different investigations, use is made herein, wherever possible, of flowfield properties as evaluated and published by the individual experimenters. In cases where such data were not available, it was necessary to compute approximate values for the momentum thickness Reynolds number Re_θ and momentum thickness θ based on the Bishop[36] and PANT[10] formulations, respectively. Bishop's formula for the sonic point Reynolds number, given by

$$Re_{\theta^*} = 3620\sqrt{P_o R_n}(H_o)^{-0.412} \text{ at } S/R_n \simeq 0.75 \qquad (2)$$

[with P_o (atm), R_n (feet), and H_o (Btu/lb)] was found, when adjusted linearly for location on the sphere (S/R_n), to compare within 10-15% of values computed for PANT test conditions using the SAANT and/or BLIMP programs.[10] Similarly, the correlation of BLIMP and SAANT solutions for the boundary-layer momentum thickness, as published by Anderson,[10] was used where necessary. The Anderson results not only provide a relationship by which the stagnation point momentum thickness ($T_w/T_o \simeq 0.4$) can be computed, namely,

$$\theta_o \text{ (in.)} = 0.5\times 10^{-5} H_o^{0.625}\sqrt{R_n/P_o} \qquad (3)$$

but his work also describes the dependence of the local momentum thickness θ/θ_o on location (S/R_n) and wall temperature (T_w/T_o).

A. Arcjet Testing

The arcjet provides transition data complementing results obtained from wind-tunnel and ballistic range experiments by

Table 2 Nosetip transition ground test data base

	PROGRAM	REFERENCE	FACILITY	M_∞	$Re_{\infty/m}$ ($X10^6$)	P_o (ATM)	$\frac{To}{3}$ ($10\ ^\circ K$)	R_n (mm)	k_{30} (μ)	$(Tw/Te)_T$	$Re_{\theta T}$	$\frac{k}{\theta}\frac{Te}{Tw}$	$\bar{x}$	
1.	REENTRY	-	-	< 24	3-300	4-300	-	-	12.7-635.	.4-1	20-800	.1-10	.1-10	
2.	PANT-A	ANDERSON, '73	NOL-8	5	3-33	.5-1.5	.7-.8	63.5,127.	40.6-1016.	.4-.8	30-130	3-70	2-10	CAL. MODEL TESTS
	PANT-J	JACKSON, '74	NOL-8	5	5-16	.4-1.2	.5-.8	19.-94.	76.2,88.9	.4-.8	25-110	3-16	2-6	
3.	ART	PHINNEY, '74	NOL-8	5,8	3-33	.1-1.4	.6-.8	63.5,127.	30.6-1016.	.4	10-110	3-80	3-15	
4.	NTEP-5	LADERMAN, '76	AEDC-B	6	7-20	.2-.6	.5	178.	152.	.95	80-110	3-5	.2-4	BL PROFILES
	NTEP-7,8	DEMETRIADES, '76	AEDC-B	6	7-20	.2-.6	.5	178.	43.2-152.	.4-.95	50-280	1-6	1-5	
5.	NOZ. WALL	DEMETRIADES, '78	FACC-SWT	< 1	1-13	.3-1	.3	297.	22.9-254.	.8-.95	150-550	.3-2.5	.3-3	NOZZLE WALL
6.	STREET-A	OTIS, '70	NOL-8	5	5-30	.6-3.2	.8	88.9	76.2	.4	35-75	4-8	3-7	CAL. MODEL TESTS
	STREET-A	BOUDREAU, '76	AEDC-F	8,12	16-164	-	.8	6.35-44.5	25.4-127.	.4	-	-	-	INDENTED
7.	AVED	HOLDEN, '77	SHK TUN	11	23-33	2.0	1.6	50.8	102.	.20	20-40	18-20	10-12	SHOCK TUNNEL
8.	NASA	DUNAVANT, '67	HWT	10,11	3-7	.1-.25	1.-1.2	76.2	203.-1270.	.25-.30	20-35	8-40	4-6	REGULAR $\bar{k}$
	(LANGLEY)	DEVEIKIS, '61	9X6 SWT	3	23-40	3-5	.6	57.2	10.2-20.3	.4-1.0	80-180	1.5-4	1.5-4	
	↓	BECKWITH, '57	9X6 SWT	2, 4.15	26-164	7-35	.3-.7	76.2	5.1	.5-1	100-350	-	-	SMOOTH; TUN. GRIT
		COOPER, '60	BWT	5	240	11	-	25.4	.08-12.7	.16-.65	-	-	-	SMOOTH; TUN. GRIT
		CHAUVIN, '57	FLT	2-5	40-66	5-18	-	112.	2.54	.6-.9	320-420	.2-.4	.2-.4	$Re_{\theta T}$ = 410
		GARLAND, '57	FLT	2-3	42-62	5-10	-	102.	2.54	.5-.9	300-600	.3-.5	.3-.5	$Re_{\theta T}$ = 555
		HALL, '57	FLT	1-3	20-59	5-10	-	102.	.51-2.54	.5-.9	900-1200	-	-	$M_T > 1$
		BUGLIA, '61	FLT	2.8	5	7.5	-	165.	.25	.68	794	.03	.03	$Re_{\theta T}$ = 794
9.	MISCEL.	DIACONIS, '74	LEWIS SWT	3.1	3-49	-	.3	17.8	.51-3.3	.6-1.6	-	-	-	$M_T > 1$
	↓	STETSON, '59	ST	1.8-2.5	-	10-7.00	-	12.7, 25.4	.10	.05-.15	200-300	.3-.8	-	LOW T_w/T_e
		BANDETTINI, '59	AMES SWT	2.5-3.5	3-16	-	-	241.	15.2-76.2	.9-1	300-600	-	-	$M_T > 1$; TUN. GRIT
		VAN DRIEST, '69	JPL SWT	2	-	-	-	82.6	102.381.	-	-	-	-	SINGLE ROW k
0.	RANGE	REDA, '79	AEDC-G	10-14	-	25-100	-	10.2-31.8	10.2-20.3	.2-.4	25-200	2-10	2-6	CLEAR AIR
	↓	SHIH, '78	AEDC-G	11-14	65-230	50-200	-	6.35	10.2-15.2	.2-.4	20-25	12-16	7-9	N_2
		WASSEL, '79	AEDC-G	12-14	30-230	25-200	-	6.35,10.2	10.2-15.2	.2-.4	15-70	5-14	4-9	N_2

measuring transition behavior for realistic nosetip materials under conditions simulating the high enthalpy and pressure loadings of re-entry. In this manner the combined effects of ablation and erosion are approximated and the material response to transition can be determined. The two most active arcjet facilities for nosetip transition studies are the High Impact Pressure (HIP) Arc Heater at McDonnell Douglas Research Laboratories (MDRL) and the Re-entry Nosetip (RENT) Facility at the Air Force Flight Dynamics Laboratory (AFFDL). The HIP facility can provide a model impact pressure of 210 atm and a bulk enthalpy of 8500 Btu/lb. The corresponding capability in the RENT facility is 100 atm and 4000 Btu/lb.

In general the arcjet has proved to be an outstanding test facility by which candidate nosetip materials can be evaluated from the standpoint of recession rate response and transition behavior. Pressure ramp testing provides results defining a material's transition performance. All investigators, however, recognize the inherent limitations associated with arcjet testing, e.g., freestream turbulence, bulk vs centerline enthalpy spike, flowfield gradients, and measurement resolution, and care is exercised to qualify measured results. Many material samples have been tested, and extensive documentation has been made of test performance data and of roughness characterization measurements for sectioned posttest samples. Because of the noted test limitations, investigators have made use of the *relative* transition performance for a given material in comparison with other potential materials under consideration. This screening capability of the arcjet has been a valuable aid to workers developing real materials for re-entry nosetips.

B. Wind Tunnel Test Data

In this section a review is made of *wind tunnel* experiments on *roughness-dominated* nosetip transition. Only results for "large" roughnesses will be discussed wherein the effect of tunnel flow disturbances on transition is considered negligible.[37] The data base spans a range in freestream Mach number, Reynolds number, nose radius and roughness height of 2-11, $10\text{-}33\times10^6$/m ($3\text{-}10\times10^6$/ft), (0.25-7.0 in.), 6.4-17.8 mm and (0.6-40 mil) 0.015-1.02 mm) , respectively. The data have all been processed and correlated in a consistent manner using the 30th percentile exceedance height definition discussed in Sec. III, and only results forward of the sonic point ($M_e<1$) will be considered.

One important aspect of the current data review was the need to perform an independent evaluation of the approach(es) taken by individual investigators in determining transition location. Although there exists, in general, favorable comparison in transition detection between surface sensors (wall temperature, heat transfer), mean flow boundary-layer measurements, and hot-wire surveys,[12] there may be data uncertainties in some measured results due to sensor distribution/location limitations or even data interpolation effects. For this reason, namely, sensitivity of transition location "measurement" to sensor spatial resolution and interpolation, a re-examination of published wall heat transfer data for rough-wall nosetip transition has been made. A consistent tangent-slope-intercept method, based on the heat transfer rise at transition, has been used throughout to specify the "beginning" of transition such that experiment-to-experiment results will correspond to the same baseline definition. Where evident, malfunctioning sensors were excluded from the data base, and results were averaged for those experiments that provided transition location data for more than one orientation ray. Transition locations (S_T/R_N) as measured herein and as quoted by the individual investigators, as well as other important test parameters for the current wind tunnel data base, are given in tabular form by Batt and Legner.[2]

PANT Results

Perhaps the most important and widely publicized set of rough-wall nosetip transition data is that generated by Aerotherm under the PANT program.[10,11,38] Extensive use of this data base has been made by many investigators to aid in development of correlation models for empirically treating nosetip transition. In this effort, both reduced data "points" and the familiar PANT location criteria given by Eq. (1) were used. In addition, many comparisons were made between "PANT" and other correlation models and experimental results because PANT has been recognized as a standard set of data.[7,8]

The popular use of the PANT measurements has taken place in spite of the fact that investigators are aware of certain limitations relative to the PANT results. For example, concern has been expressed over such issues as data sensitivity to freestream disturbances,[10,39,40] potential differences in correlation slope (n) between location data ($n\simeq-0.7$) and movement results ($n\simeq-1.5$), and the indication that the correlation criteria based on the $n=-0.7$ power corresponded to a shallower slope than that inferred from other data. The distinction between "location" data and "movement" data is as follows: Location data are the ensemble of the entire transition data base, whereas movement data refer to the transition for a specific configuration (run) in which only one parameter, such as T_w or tunnel stagnation pressure, varies. The ballistic range data of Reda[5] further emphasized this slope issue, since Reda's real-material test results corresponded more nearly to a correlation slope, in PANT coordinates, of $n=-1.3$. For these reasons, therefore, a detailed re-evaluation of the PANT data base has been undertaken herein.

Typical heat transfer distribution curves for one of the PANT nosetip models are shown in Fig. 4a. Note that the data points plotted in this figure in combination with the tangent-slope-intercept method for determining transition onset (based on the sudden heat transfer increase at transition) provide a good definition of transition location. This approach, however, requires some interpolation and becomes sensitive to the availability and spacing of heat transfer sensors, as can be seen by examining another sample of PANT test data given in Fig. 4b. Shown therein are designated transition locations and interpolated results as determined under the PANT program and as revised herein. The revised data differ from PANT's original transition locations primarily as a result of a more consistent application of the tangent-slope-intercept approach in terms of temperature gradient at transition and optimal use of measured data points. At the very least, this difference in interpolation scheme should be treated as an upper-bound technique for measuring S_T/R_N locations, since the revised slopes all tend to be steeper and thus shift the transition location to higher S_T/R_N values. The heat transfer plots for all the other run cases of the Series A and J experiments have been analyzed similarly. General agreement between the two methods of interpolation exists for most S_T/R_N values. However, for some cases, differences are in evidence which are significant in interpreting the *movement* of transition with wall temperature increase.

This latter point is illustrated by comparing transition data from the two methods in terms of PANT's familiar transition parameters, Re_θ vs ψ (Fig. 5). The revised results shown do *not* include PANT's low roughness height data [$k=.015$ mm (0.6 mil)] because these data are considered influenced by tunnel disturbance effects. These "adjusted" data suggest that a correlation slope n based on transition movement for *each* run case is substantially larger than the $n=-0.7$ value associated with PANT's baseline correlation model. This implies that, although use of the baseline criterion would provide a reasonable approximation to the "general" location of transition, it would not describe the appropriate *movement* (progression) behavior. This result is also suggested by the

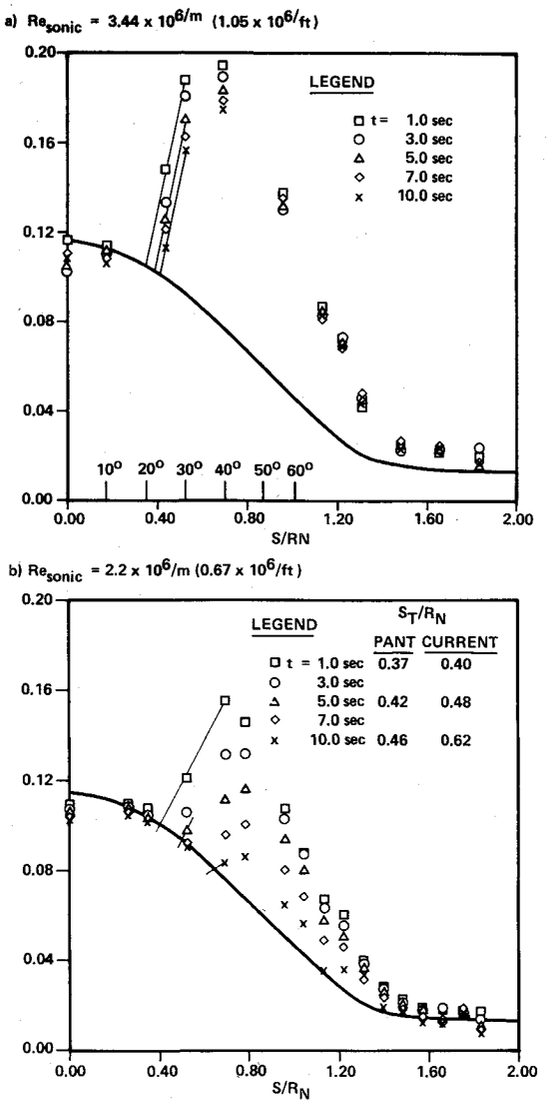

Fig. 4 Transitional heat-transfer distributions—PANT Series J (R_n = 3.5 in., 88.9 mm; k = 3.5 mil, .089 mm; Ref. 9).

original PANT data base [cases 113, 163, 165, 171, and 174 (Fig. 5a)] which implies $n \sim -1.5 \pm 0.1$ rather than the commonly quoted $n = -0.7$ value. Demetriades[9] discusses this issue of "detailed (fine) structure of transition movement" and points out clearly that what may seem to be scatter on a global basis is in fact important data trends reflecting the structure and movement of transition. The current revision to the PANT transition data base not only is within the uncertainty ranges of the raw data measurements, but seems to provide results more consistent with other transition movement data.

The revised data in PANT coordinates (Fig. 5) are seen to separate out into individual run cases, apparently as a function of nose radius and/or roughness height. This trend is also evident[2] in results from the ART[41] experiments and Demetriades nozzle wall[9] experiments.[2] Van Driest et al. similarly observed this effect in his sphere cone experiments[42] and attributed such a data trend to the stabilizing effects of wall curvature. Other investigators[41,43,44] have similarly concluded that this phenomenon is an important factor in nosetip transition and have included van Driest's curvature correction term in the definition of the effective surface roughness, namely,

$$\bar{k} = \frac{k}{1 + 350\, k/R_n} \tag{4}$$

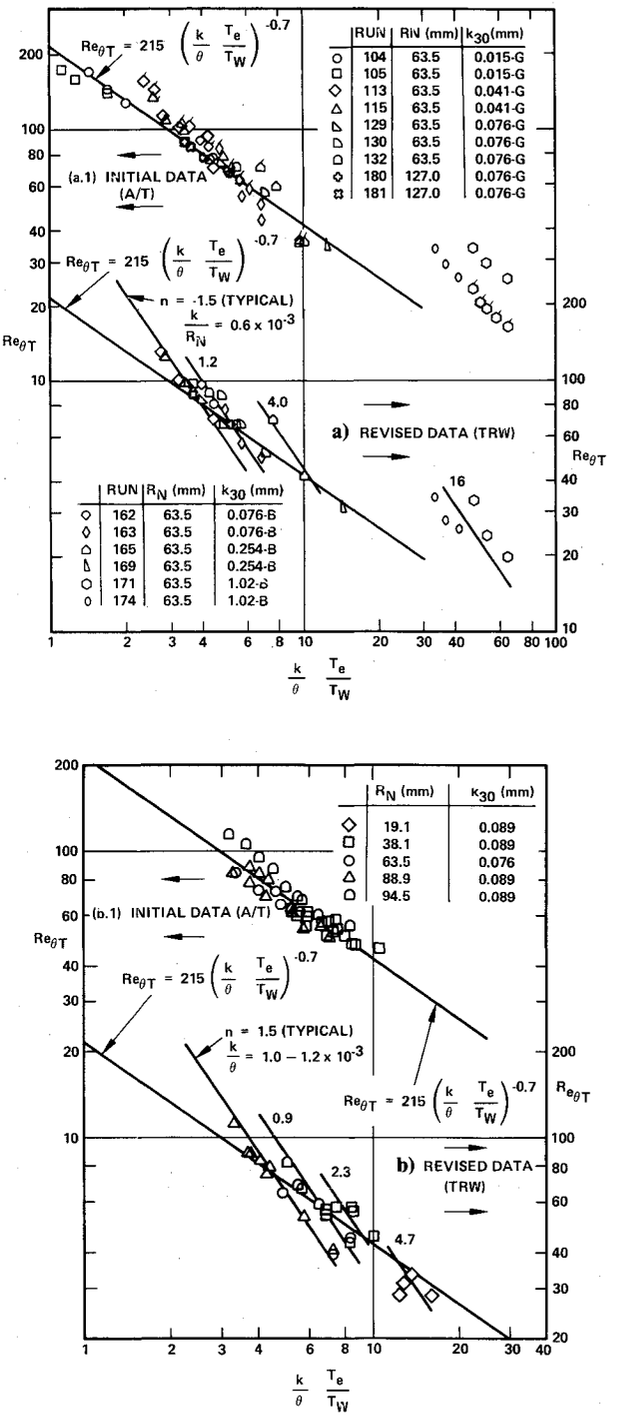

Fig. 5 Transition correlation in PANT coordinates. a) PANT Series A, b) PANT Series J.

A replotting of the PANT data base of Fig. 5 in terms of van Driest's effective roughness is given in Fig. 6, and a general collapse of the data to within a ±30% uncertainty band is evident. A correlation to the results shown is given by

$$Re_{\theta T} = 500 X^{-1.5} \tag{5}$$

where

$$X = \frac{\psi}{1 + 350\, k/R_n}$$

is a curvature-corrected disturbance parameter.

This successful data correlation using a wall curvature term, it should be noted, has already been pointed out earlier

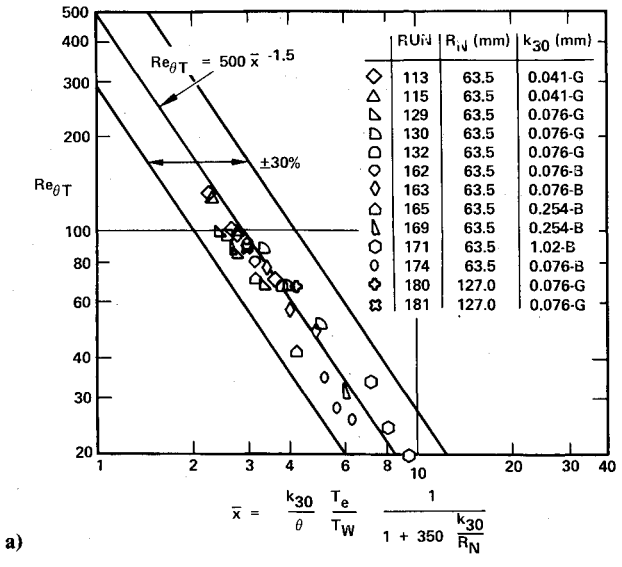

a)

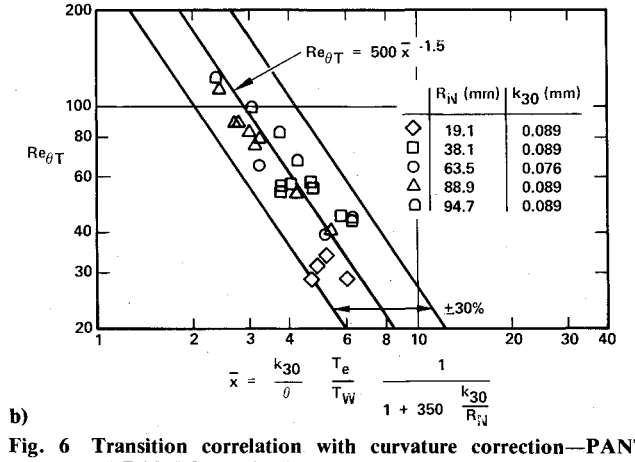

b)

Fig. 6 Transition correlation with curvature correction—PANT program: a) PANT Series A; b) PANT Series J.

by other investigators. However, the important point in the present formulation is that now both location *and* movement curve slopes are the same, namely, $n \simeq -1.5$. In the original formulation of the PANT transition criterion, data trends (correlation slopes) exhibited by some individual run cases were inconsistent (steeper) relative to the empirically fitted transition curve, in part because of inclusion of PANT's low roughness height data and some transition location results that were sensitive to the interpolation uncertainties. Note that the correction term remains constant for a given run case in the present correlation model. Thus, *curve slopes* for individual run cases remain unchanged in transferring data from the Fig. 5 to the Fig. 6 format.

In light of the favorable comparison shown in Fig. 6 and recognizing that the basic data base has inherent accuracy limitations, it would appear that extensive comparison with other transition criterions[5,14,19,22,34] may not be particularly fruitful. Also the formulation, Fig. 6, seems attractive from the standpoint that it makes use of integral boundary-layer properties rather than depend on detailed calculations of boundary-layer profile properties. This latter procedure is necessary for those models that require flow properties at the height of the surface roughness elements,[10] an approach that may compound uncertainty effects because of difficulties in proper characterization of surface roughness (Sec. II).

Other Rough-Wall Nosetip Transition Data

An integral part of this review effort was the evaluation of the many sets of wind tunnel results on rough-wall nosetip transition. It as found that some of the data were obtained with models whose surface roughness characterization was poorly quantified[45-47] or with models corresponding to biconic and/or nonhemispherical shapes.[48,49] In addition, in other cases[46,50] it was determined that transition occurred on the frustum and/or downstream of the model's sonic line (Demetriades Cap IV A, Adiabatic[12]). Since the present study emphasizes subsonic transition on hemispherically shaped nosetips, such "other" data have not been used in developing a transition correlation model. The "selected other" data sources that were found to provide useful results on rough-wall nosetip transition are Deveikis,[25] Dunavant,[31] Street A (Otis[51]), Holden,[52] ART (Phinney[41]), NTEP (Laderman,[44] Demetriades[12]), and Demetriades.[7,9]

Summarized transition data for these latter experimental studies, excluding the results of Demetriades nozzle wall experiments that have already been documented,[9] are also given by Batt and Legner.[2] The noted listing includes author-specified data as well as results derived herein for roughness heights (30th percentile value, Sec. III) and transition locations based on the tangent-slope "measurement" technique. A combination of different test facilities was used to obtain the noted data. This data base covers a wide range of Mach number (2-11) and provides nearly an order of magnitude variation in the transition disturbance parameter $1.5 \leq X \leq 10$, where X is as defined in Eq. (5). This is evident in Fig. 7, which illustrates that favorable comparison also exists between the present correlation model in Eq. (5) and both the ART results, based on the current reduction of initial heating rate data and on "other" transition data. The ART data further illustrate the manner in which transition "progresses" *forward* with increasing Reynolds number, a movement trend identical to the behavior of nosetip transition during re-entry. Such data therefore provide an important set of results complementing the more commonly acquired progression data based on wall temperature increase and the corresponding *aft* movement of transition. Note that the low roughness data of Demetriades[9] (Fig. 7c) provide an important contribution to nosetip transition since they fill in what had been a major gap in the overall data base, namely, measured results describing the "knee" portion of the transition correlation. These more recent data appear to fair into the smooth-wall-limit results to be discussed shortly in Sec. IV. C.

Wind Tunnel Data Summarized

Of obvious interest in correlating data from different sets of measured results is the suitability of the selected correlation when compared with the combined or overall data base. For this reason, in Fig. 8, all wind tunnel and free-flight data discussed heretofore are summarized. Also indicated in Fig. 8 is the suggested correlation model, based on the present work, which is given by

$$Re_{\theta T} = \begin{cases} 500\,X^{-1.5}, & X \geq 1.0 \\ 500, & X < 1.0 \end{cases} \tag{6}$$

where

$$k = k_{30}\ (30\%\ \text{exceedance height})$$

It is seen that the indicated correlation provides a reasonable representation for the available data base, not only in terms of onset location but also with regard to the movement of the transition front. When Demetriades[9] presented a similar plot for his nozzle wall data, there existed a disparity between the PANT correlation model, with its $n = -0.7$ slope, and the movement data for each run case ($n \simeq -1.5$), a result Demetriades also pointed out. The AVCO correlation (Chen et al.[39]) as modified for curvature is also indicated in Fig. 8. The close agreement between AVCO's correlation and the

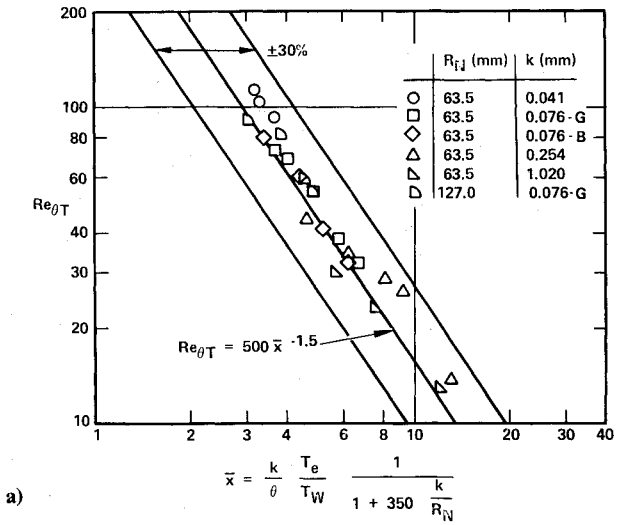

a)

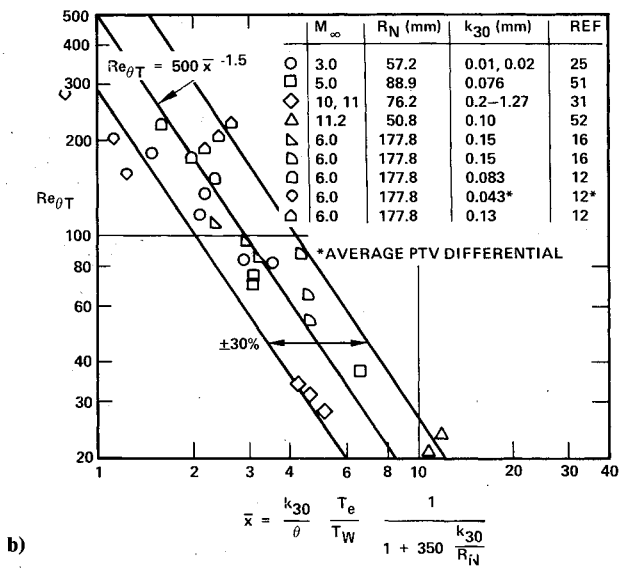

b)

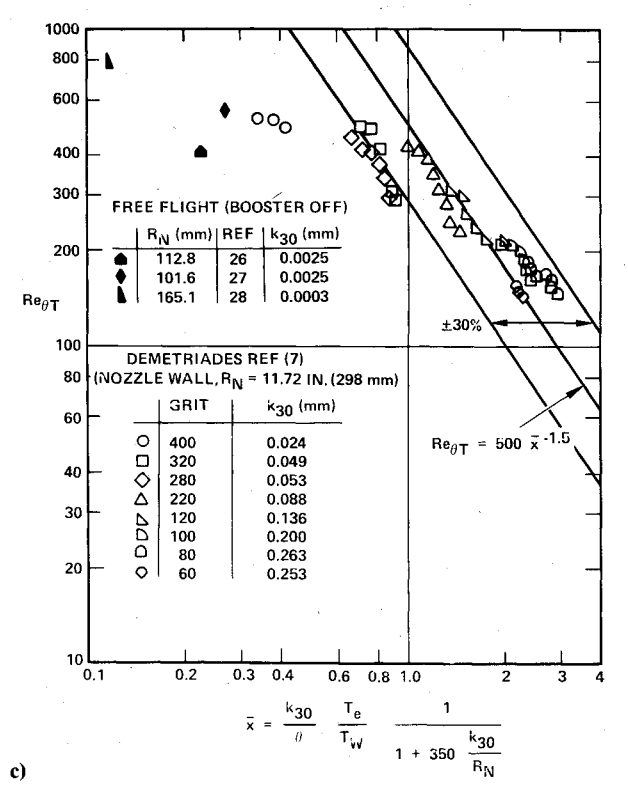

c)

Fig. 7 Transition correlation with curvature correction: a) early-time ART data ($M_\infty = 8$, Ref. 41); b) "other" wind-tunnel data (Batt and Legner, 1980); c) Demetriades[7] nozzle wall data; free-flight data.

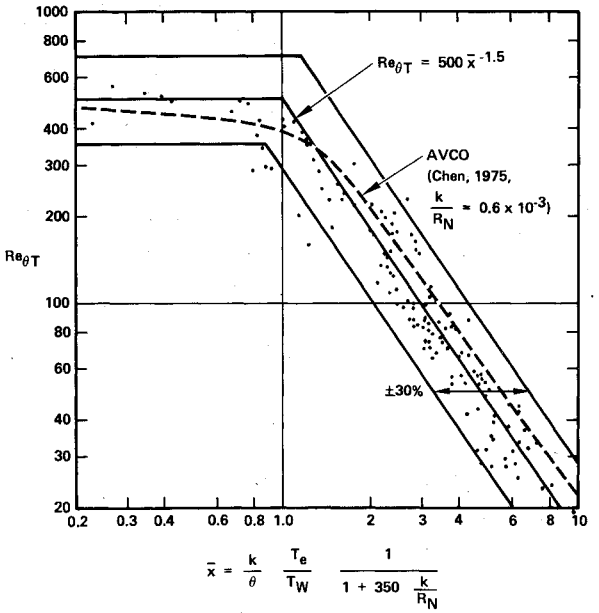

Fig. 8 Summarized wind-tunnel data correlation.

current work's *independent* assessment of ground-test transition data is considered an important finding.

C. Smooth-Wall Blunt-Body Results

Workers investigating smooth-wall blunt-body transition under high-speed conditions[3,29,40] have made use in their correlation analyses of wind tunnel and free-flight data as well as X-17 re-entry flight results.[53,54] There is general agreement that wind tunnel transition measurements are sensitive to freestream disturbances and that care must be exercised in interpreting reduced data. The significance of this well-known qualifier was clearly demonstrated by Dryden in his review of flat-plate transition.[37] Also White's smooth-wall correlation summary[40] illustrated that wind-tunnel-derived transition Reynolds numbers ($Re_{\theta T}$), although displaying the expected sensitivity to edge Mach number, were substantially lower than undisturbed free-flight results. Several wind-tunnel investigators[45-47] have similarly referred to the unavoidable problem of tunnel grit that quickly roughened up their "smooth" models (1 to 5-mil pit holes) in the vicinity of the stagnation point.

The smooth-wall limit to blunt-body transition is an *essential* element in any transition correlation model. In this paper only those data that correspond to undisturbed freestream conditions and smooth-wall-limit surface properties are considered. Thus various wind tunnel results[45-47] including Street A and PANT data have *not* been used in the present evaluation of the smooth-wall $Re_{\theta T}$.

Smooth-wall transition results from wind tunnels and other sources are summarized in Table 2. Here one observes that the results from the wind-tunnel experiments are low compared with data measured in free-flight testing or in the "quiet" tunnel studies[9] of Demetriades.

The primary sources for smooth-wall-limit data for blunt-body transition in *free flight* are Refs. 26-28. All experiments were performed at the Langley Pilotless Aircraft Research Station, using two-stage rocket test vehicles. Hall et al.[56] performed similar testing with a "super" smooth nosetip vehicle; however, his results revealed that transition occurred downstream of the sonic line. Measured rms surface roughnesses were 0.8, 0.6, and 0.6 μm (0.003, 0.025, and 0.025 mil) test models of Refs. 26, 27, and 28, respectively. Flight Mach numbers varied from 2.0 to 5.0, and the transition disturbance parameter X [Eq. (5)] was ≤ 0.3, well within the smooth-wall-limit domain. $Re_{\theta T}$ varied from 250 to 800 and showed sensitivity to booster motor vibration effects. This latter result is illustrated by the summary data of Table

2, which indicate that coast- and/or sustainer-only data correspond in general to higher $Re_{\theta T}$ ($\simeq$400-800) than do booster-on results.

The present free-flight data are plotted in Fig. 7c, wherein only booster-off results are shown. The significant feature of these data is the relatively *high* values for measured transition Reynolds numbers. These data thus suggest that the smooth-wall-limit value for $Re_{\theta T}$ is a value as large as $500 \pm 30\%$ rather than the lower wind-tunnel-observed value (200-300). This finding is an important result of the free-flight test program since transition onset during re-entry occurs at values of the disturbance parameter (x) of the order of 1, that is, the knee location of the transition correlation. Since the movement of transition "tracks" along the correlation curve, any misalignment of the smooth-wall limit will have a substantial impact on transition progression just after onset. With the data discussed in Sec. IV.A, the summary results of Fig. 9 suggest a curve slope at $x \simeq 1$ of $n = 1.5$, which corresponds to a significantly "faster" transition movement than would be the case if the knee portion of the curve were based on a value of $Re_{\theta T}$ (smooth) $\simeq 300$.

A unique set of "smooth"-wall blunt-body transition data[9] has been measured by Demetriades[9] using the throat region of a supersonic nozzle wall as a blunt-body simulator. This flowfield retains many of the important features of high-speed flow over a hemisphere, including curvature, pressure distribution and gradient, and the increasing-decreasing unit Reynolds number. By bonding selected samples of sandpaper overlays, experimental data were measured over a range of disturbance parameter x from 0.1 to 2.0. This range in x extends well into the smooth wall domain and because of the absence of supersonic noise effects, which are the major source of tunnel flow disturbances in conventional wind tunnel experiments, the data correspond essentially to disturbance-free, or "quiet," tunnel measurements. These transition measurements are plotted in Fig. 7c using the k_{30} height definition. The data illustrate, as originally pointed out by Demetriades, that the PANT-type transition criteria do not hold at the low range of the disturbance parameter ($x \lesssim 1$) and that a smooth-wall $Re_{\theta T}$ limit of the order of $\simeq 500$ is appropriate.

D. Ballistic Range Test Data

Since the pioneering work by Reda[57] in development of the hyperballistic range as an important tool in nosetip transition research, numerous experiments have been performed in the Naval Surface Weapons Center (NSWC) 1000-ft range as well as in Arnold Engineering Development Center's (AEDC) Range G facility. Surface-temperature data, as measured by electropyrometry, have provided important results demonstrating the dependence of nosetip transition on such flowfield and/or model parameters as freestream conditions, nose radius, wall temperature, surface roughness, material type (graphite vs carbon-carbon weave), and test gas (nitrogen vs clear air).

Most recently, all ballistic range testing has been carried out in Range G, where the combined efforts by Reda, Shih/Wassel (SAI), and Raper (AEDC) have led to development of the ballistic range as an essential nosetip test facility. Transition data, for example, are now available under real-gas conditions at high Reynolds numbers and for realistic nosetip materials. As such, these more recent data complement conventional wind-tunnel data and serve as an important link to the full-scale flight-test problem.

Free-flight and tract-guided nosetips have been tested in Range G, all at zero angle of attack, with model sizes from 6.4 to 31.8 mm (0.25 to 1.25 in.) in nose radius. Experiments have been performed with both smooth- and rough-wall tungsten models and preablated real-material nosetips, such as ATJ-S, Graphnol, and CMT graphites plus carbon-carbon weave materials (FWPF, 223). Prior to testing, all real materials models are preablated under low-pressure laminar heating

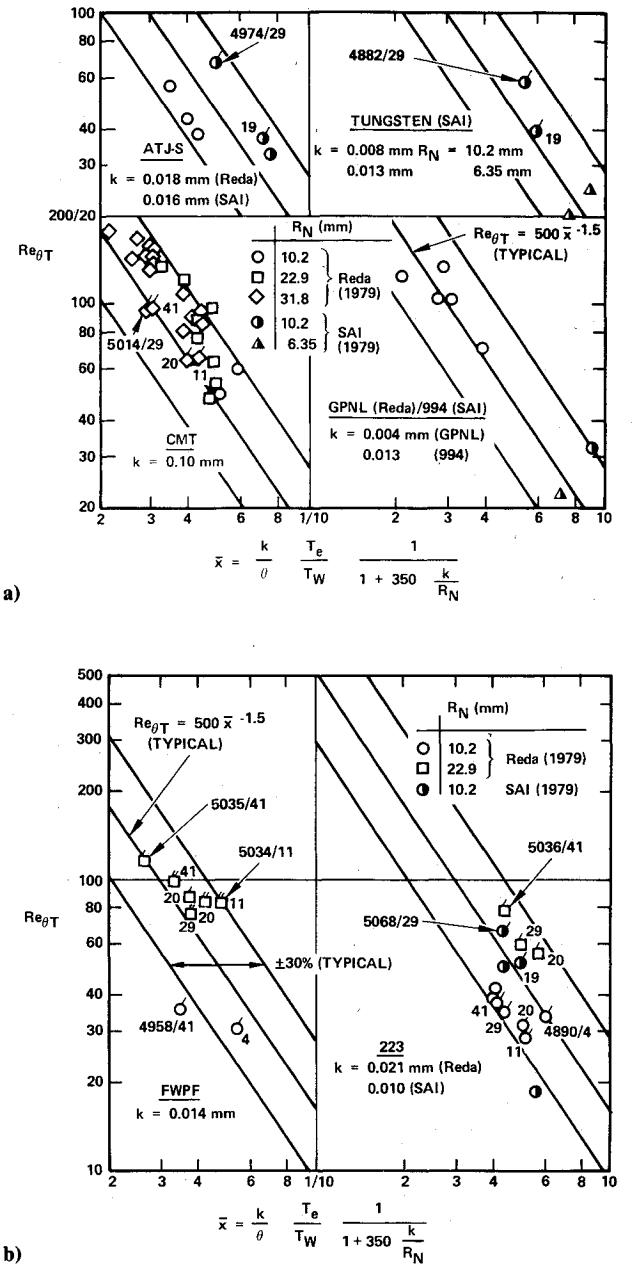

Fig. 9 Transition correlation with curvature correction—ballistic range data: a) graphites; b) carbon-carbon weaves.

environments in order to simulate heating effects and corresponding laminar surface roughnesses associated with pretransition, high-altitude re-entry. The photopyrometer measurement technique operates by recording on film both known and unknown temperature sources, and through the use of an established calibration relationship between source brightness temperature and film density a determination is made of surface-temperature distribution. An image converter camera (ICC) photograph typically provides an image of the relatively "cool laminar" island in the vicinity of the stagnation point surrounded by a zone of transitional/turbulent heat transfer. Posttest processing of each image converter negative is made by an isodensitometer that defines relative film density as a function of surface location.

All ballistic range transition results were determined from surface-averaged data using a positive-slope-change approximation to the transition location (S_T/R_n) based on either surface temperature (Reda) or heat-transfer distribution (SAI). In some cases the (S_T/R_n) locations selected for use herein were somewhat larger than values determined by Reda or Shih, in part because of the use of a tangent-slope ap-

proximation consistent with the wind-tunnel data processing approach of Sec. IV.A. Reda[5] gives a detailed listing of his clear air results, and summarized SAI data (Shih,[13] Wassel,[14] nitrogen) as used herein are presented in Ref. 2.

Ballistic range data for the Reda and SAI measurements are summarized in Fig. 9 in terms of the momentum-thickness Reynolds number and the PANT disturbance parameter X as modified for curvature effects. The data include results for both nitogen[13,14] and clear air[5] test gases correspond to characteristic roughness heights as specified in Sec. III. The results are separated into material type, with the open symbols representing the Reda results and the half closed symbols the SAI data. Shown also in the plots of Fig. 9 are flag-designated points to illustrate the typical movement of transition with range station and the wind-tunnel data fit correlation given previously by Eq. (6). Note that, in achieving the favorable correlation evident in Fig. 9, the Reda and SAI values for ATJ-S roughness heights as used are in general agreement, whereas selected surface roughnesses for 223 differed by about a factor of 2. This apparently anomalous behavior in the characteristic roughness magnitude for real-material nosetips as tested in the ballistic range is considered a significant result of the range experiments and a potentially important clue toward improved understanding of nosetip transition. Note, for example, that the bulk graphite results of Reda in clear air (with ablation) and the data of SAI in nitogren (without ablation) show that, in general, good correlation exists between pretest-measured roughnesses and established transition criteria. This agreement is therefore consistent with the finding that ATJ-S roughnesses, in the absence of such macroroughness effects as scalloping and gouging, are in general relatively insensitive to laminar or turbulent heating environments and thus ablation will have a negligible influence on the characteristic surface roughness. Preablated graphite nosetips in a low-pressure arc environment (Aerotherm's Plasma Arc Generator) or the AFFDL's 50-MW RENT facility should therefore provide the same surface roughness characteristics and the same corresponding transition behavior in either nitrogen or air.

Conversely, transitional measurements for Reda's orthogonal-weave materials (223 and FWPF) demonstrate that pretest roughnesses produced by low-pressure arcjet preconditioning need to be increased by approximately a factor of 2 in order for reduced data to compare favorably with available transition criteria. Furthermore, the resultant roughness heights [$h_{223} \simeq 0.021$ mm (0.84 mil), $h_{FWPF} \simeq 0.010$ mm (0.54 mil)] are substantially larger than roughnesses as "inferred" from re-entry drag data based on transition-onset altitude. Because of these discrepancies, a review was made of available RENT data on characteristic surface roughnesses for 223 and FWPF materials.

Interestingly enough, it was found that 223 and FWPF roughness height distributions for the Reda/Shih *low*-pressure ablated models (Aerotherm arcjet) were significantly *lower* than corresponding measurements for models ablated in the 50-MW RENT facility, even for laminar environments. The differences are tentatively believed caused by the high loadings ($P_o \sim 50$ atm) and corresponding severe ablation effects associated with the RENT facility as compared with the low stagnation pressure (~ 0.1 atm) at which Aerotherm's arcjet facility operates. During ballistic range testing, however, nosetip stagnation pressures may be of the order of 50 atm. In addition, because of wall temperature effects and flowfield dependence on range station, the transition line *moves aft* with time and range station (see Run 4890, Fig. 9b). Because the Reda experiments were all performed in clear air, some surface ablation and/or high pressure-induced material erosion occurred during testing. This aspect of ballistic range testing in clear air was originally pointed out and reviewed by Reda in his pioneering experiments with graphite nosetips in NSWC's 1000-ft range.[58] Thus the local roughness character triggering transition may be more typical of RENT-type preablated models than of those models treated in Aerotherm arcjet facility. This candidate explanation is supported by recent Range G data in *nitrogen* by SAI (Fig. 9b), wherein pretest 223 roughness heights were found to be consistent with flight *and* ballistic range transition-onset values. For the purposes of the correlation analysis presented herein, therefore, the Reda 223 and FWPF data correspond to RENT induced high pressure environment roughnesses whereas the SAI results for 223 are based on the roughness characteristics consistent with low-pressure precondition testing.

In general, the data of Fig. 9 compare well with the correlation criteria derived from the wind-tunnel transition data. Within the noted uncertainty band ($\pm 30\%$) the data are seen to account for the effects of boundary-layer flow properties, wall temperature, nose radius, material type, and roughness height. Separating out the data into material type, the Reda CMT results were found to correlate better when the curvature correction term was retained in the definition of the disturbance parameter than when it was not included. Also, those few shots for which measured data are available at several range stations (numbers 4890, 5014, 5036, and 4974) illustrate that the transition movement (progression) is consistent with a correlation slope to the -1.5 power in agreement with the overall data correlation curve fit. As such the Reda/SAI range data represent an important verification of the wind-tunnel results discussed in Sec. IV.B. The satisfactory correlation of this real-material, high-pressure, real-gas data base with the noted correlation (Fig. 10) provides increased confidence in applying the present correlation model to nosetip transition during re-entry.

V. Nosetip Transition Correlation

The systematic review and evaluation herein of the ground-test data base on nosetip transition has resulted in a consistent description of the phenomenon. Available results from many investigations, including wind tunnel *and* ballistic range data, have been assembled and correlated in terms of a common roughness height definition based on the 30% exceedance height value. The combined data set suggests a correlation given by

$$Re_{\theta T} = \begin{cases} 500\,X^{-1.5}, & 1 \le X \le 10 \\ 500, & X < 1 \end{cases} \tag{7}$$

where

$$X = \frac{k}{\theta}\,\frac{T_e}{T_w}\,\frac{1}{1+350\,k/R_n}$$

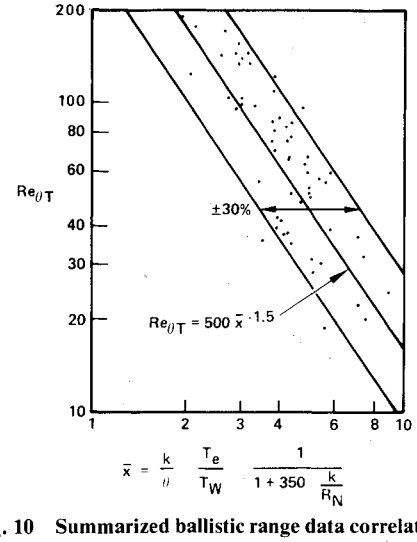

Fig. 10 Summarized ballistic range data correlation.

This best-fit correlation agrees with the data to within ± 30% for the range of X of $0.1 \leq X \leq 10$. This agreement not only exists in terms of transition onset for the cited X range for the many different sets of data but also is consistent with the *local* movement and progression of transition with wall temperature and/or Reynolds number. For $X \leq 1$ a constant smooth-wall-limit value of $Re_{\theta T} = 500 \pm 30\%$ is recommended.

Although the transition correlation described here was established during the present review, it should be noted that correlation models similar to Eq. (7) were suggested and/or implemented by earlier investigators. Swigart discovered that a correlation law to the $-3/2$ power seemed to fit available data well[43] when the displacement thickness δ^* was used rather than θ. Also, Chen et al.[39] pointed out that a correlation curve slope much steeper than the original PANT model was appropriate. These workers found that the slope for $X > 1$ was bracketed between a -1 to -2 law, with their final recommended value being $n \simeq -1.35$. Van Driest, of course, must be given full credit for his curvature correction term, which accounts in an approximate but effective manner for the stabilizing effects of local centrifugal forces. Finally, the latest results of Reda[5,8] and Demetriades (nozzle wall experiments[7,9]) each illustrate that in both transition onset and/or movement a transition law incorporating a stronger dependence of transition on the local disturbance parameter was required. Reda recommended a data slope of $n = 1.3$, whereas movement results from Demetriades' experiments are well represented by $n \simeq -1.5$.

A physical rationale for the correlation (7) can be obtained by appealing to the critical Reynolds number approach. The central idea is that, at some transition Reynolds number Re_t, the wake of an obstacle—the roughness element (cylinder, sphere, etc.) in a uniform stream—undergoes transition. Transition in the wake is preceded by oscillation of the wake at some lower "critical" Reynolds number, $Re_c < Re_t$. For a circular cylinder $Re_c \simeq 40$. If Re_c is associated with the Reynolds number $Re_k \equiv \rho_u U_k k/\mu_k$ at the top of the roughness element, i.e., $Re_c = Re_k$, then it is possible[59] to write the momentum-thickness Reynolds number Re_θ in terms of the flow parameters and $Re_k = Re_c$. The relationship for Re_θ can be approximated in two roughness regimes: k relatively large ($> \theta$) and k relatively small ($< \theta$). The results of these approximations are very appealing.

When k/θ is relatively large. $Re_{\theta T}$ can be shown to be proportional to $(k/\theta)^{-1}$. This $n = -1$ behavior was evident in an early displacement-thickness (δ^*) version of the PANT correlation and in the van Driest correlation. The analysis and approximations for the smaller values of k/θ are somewhat more complex; however, one can show that, in this case, $Re_{\theta T}$ is proportional to ψ^{-2} (or X^{-2}). This slope is even steeper than our data-derived $n = -1.5$. If one combines the inverse linear behavior with the inverse quadratic behavior,[60] one obtains a transition correlation with a common slope between -2 and -1. The dash line in Fig. 9 is the AVCO correlation, which appears to represent the transition data with a slightly shallower slope than the present $n = -1.5$. Further analytical work is warranted using the critical roughness Reynolds number approach for the separate roughness regimes. In the Demetriades nozzle wall experiments[7] there are strong observations that the $n = -2$ behavior occurs at small roughness and the $n = -1$ variation occurs at large roughness. At intermediate roughness values, a gradual "transition" between these slopes is evident.

VI. Conclusions and Recommendations

A. Conclusions

Several key conclusions result from the present study of roughness-dominated nosetip transition:

1) The roughness height used to characterize the surface topology and to quantify the appearance of transition must be standardized. We have chosen a common height k_{30} in order to reanalyze available data. The quantity k_{30} was determined by a technique (Sec. III) that quantifies the location for a baseline reference surface in lieu of "arbitrarily" selecting an optically apparent surface.

2) Transition data must be evaluated from many points of view. Judicious review of the applicability of a specific data set to the entire data base is often critical. The tunnel-disturbance-sensitive small-roughness PANT data [$k = .015$ mm (0.6 mil)], for example, had an unfortunately strong influence on the PANT correlation. Re-evaluation of transition point locations using more appropriate criteria was also an essential aspect of present work.

3) Use of qualified transition data together with a standardized roughness height definition led to a new, consistent presentation of the available ground-test transition data base. The current approach effectively collapsed the ballistic range, free-flight, and wind tunnel data into a common correlation formula. The present correlation model *consistently* matches observed data trends in terms of transition onset *and* movement/progression, a result not always evident in previous correlations.

4) The present review effort appears to resolve an important question regarding an observed disparity between wind tunnel and ballistic range transition data. A reprocessing of some measured results has shown that data uncertainties with regard to tunnel disturbances, transition location, and/or roughness height definition are in part responsible for the noted discrepancies. The revised data base shows that the two sets of data agree favorably when correlated by the transition model developed herein.

B. Recommendations for Future Study

In outlining the recommendations that follow, we will repeat some recommendations made earlier by other investigators. This is necessary since some issues on nosetip transition, although already pointed out, have yet to be resolved. The specific recommendations for future study are as follows:

1) The one major flaw in the current data base on nosetip transition is the lack of consistent and complete data on surface roughness characterization. Proper roughness characterization for each model's surface is therefore essential prior to future experiments on nosetip transition. It is recommended that, for each model, profilometer *as well as* microscopy-type surface roughness measurements be made. For the wind tunnel models, treated metal specimen samples identical to test models can be prepared and thereafter used for microscopy measurements. Consistent with this need for documented roughness data is the further recommendation to re-examine the raw surface roughness data that were measured on earlier programs but have yet to be processed, reduced, or published. One issue a reprocessing of these data could resolve is the relationship between element height exceedance profiles and profilometer data. An attempt has been made herein to bridge this gap, by use of a 30% exceedance height definition, but this effort has been limited by the scarcity of measured surface roughness data.

2) Further ballistic range testing of real-material nosetips, which complement and extend other experimental results, should address the important technical tradeoffs between testing in clear air and in nitrogen and the question as to whether RENT or Aerotherm's arcjets represents the best simulation of the laminar environment associated with high-altitude re-entry. Future ballistic range testing should also address the need for data spanning a wider range of disturbance parameter variation.

3) Often existing data on nosetip transition are of doubtful use because of tunnel-disturbance phenomena. Future wind-tunnel experiments should therefore be able to *demonstrate* that experimental results correspond to *roughness-dominated* transition.

4) The fact that carbon-carbon weave simulation tests have

not been performed to date under wind tunnel test conditions is also an important weakness in the available data base on nosetip transition. Investigators, for example, are without calorimeter data quantifying the dependence of nosetip transition on such roughness characteristics as macro/microroughness height magnitudes, weave spacing, and preferred weave direction.

5) Additional analytical studies are warranted in order to clarify the treatment of nosetip transition. Such studies should be directed toward developing a practical or engineering solution to nosetip transition leading to a correlation that is responsive to the needs of the flight performance analyst and is based upon physically sound mechanisms. In this regard the critical Reynolds number approach as outlined in Sec. V should be expanded to include the effects of blowing, curvature, and freestream disturbances.

References

[1] Wilkinson, H.R., private communication, TRW, 1979.

[2] Batt, R.G. and Legner, H.H., "A Review and Evaluation of Grount Test Data on Roughness Induced Nosetip Transition," TRW Defense and Space Systems Group, Redondo Beach, Calif., Final Report BMD-TR-81-58, Oct. 1980.

[3] Anderson, L.W. and Bartlett, E.P., "Boundary Layer Transition on Reentry Vehicle Nosetip with Consideration of Surface Roughness," Acurex Corp., Mountain View, Calif., TM-79-1, July 1971.

[4] Dirling, R.B., Jr., et al., "The Effect of Transition and Boundary Layer Development on Hypersonic Reentry Shape Change," AIAA Paper 75-673, 1975.

[5] Reda, D.C., "Correlation of Nosetip Boundary Layer Transition Data Measured in Ballistics-Range Experiments," AIAA Paper 80-0286, 1980.

[6] Finson, M.L., "An Analysis of Nosetip Boundary Layer Transition," Air Force Office of Scientific Research, TR-76-1106, Aug. 1976.

[7] Demetriades, A., "Roughness Effects on Boundary Layer Transition in a Nozzle Throat," *AIAA Journal*, Vol. 19, March 1981, pp. 282-289.

[8] Reda, D.L., "Correlation of Nosetip Boundary-Layer Transition Data Measured in Ballistics-Range Experiments," *AIAA Journal*, Vol. 19, March 1981, pp. 329-339.

[9] Wool, M.R., "Interim Report—Passive Nosetip Technology (PANT) Program, Vol. X. Summary of Experimental and Analytical Results (May 1973 to December 1974)," Acurex Corp., SAMSO-TR-74-86, Jan. 1975.

[10] Anderson, A.D., "Analysis of PANT Series A Rough Wall Calorimeter Data, Part II: Surface Roughness Effects on Boundary Layer Transition," Acurex Corp., Aerotherm Rept. 73-81, 1973.

[11] Jackson, M.D., "Interim Report—Passive Nosetip Technology (PANT) Program, Vol. XV. Roughness Induced Transition on Blunt Axisymmetric Bodies—Data Report," Acurex Corp., SAMSO-TR-74-86, April 1974.

[12] Demetriades, A., "Nosetip Transition Experimentation Program, Final Report, Vol. II," Ford Aerospace and Communication Corp., SAMSO-TR-76-120; July 1977.

[13] Shih, W.C.L. et al., "Evaluation of Reentry Vehicle Nosetip Transition and Heat Transfer in the Hyperballistics Range," Science Applications, Inc., El Segundo, Calif., SAI-79-541-LA, July 1978.

[14] Wassel, A.T. et al., "Evaluation of Reentry Vehicle Nosetip Transition and Heat Transfer in the AEDC Hyperballistics Track G," Science Applications, Inc., El Segundo, Calif., SAI-063-80T-014-LA, March 1979.

[15] Dahm, T.J. et al., "Passive Nosetip Technology (PANT II) Program, Vol. I: Inviscid Flow and Heat Transfer Modeling for Reentry Vehicle Nosetips," Acurex Corp., SAMSO-TR-77-11, Oct. 15, 1976.

[16] Laderman, A.J., "Effect of Surface Roughness on Blunt Body Boundary-Layer Transition," *Journal of Spacecraft and Rockets*, Vol. 14, April 1977, pp. 253-255.

[17] Anderson, A.D., "Evaluation of Theoretical Methods for the Prediction of Nosetip Boundary Layer Transition," Acurex Corp., Aerotherm TM-75-77, Aug. 1975.

[18] Wilcox, D.C. and Chambers, T.L., "Effects of Surface Heat Transfer on Boundary Layer Transition," DCW Industries, AFOSR-TR-75-1398, July 1975.

[19] Finson, M.L., "A Reynolds Stress Model for Boundary Layer Transition with Application to Rough Surfaces," Physical Sciences, Inc., Woburn, Mass., PSI TR-34, Aug. 1975.

[20] Merkle, C.L., "Stability and Transition in Boundary Layers on Reentry Vehicle Nosetips," Flow Research Rept. 71, June 1976.

[21] Merkle, C.L. et al., "An Analytical Study of the Effects of Surface Roughness on Boundary Layer Transition," Flow Research Rept. 40, Oct. 1974.

[22] Anderson, A.D., "An Evaluation of the Van Driest and Dirling Rough Wall Transition Data Correlation," Acurex Corp., Jan. 1976.

[23] Powars, C.A., "Analysis of PANT Series A Rough Wall Calorimeter Data, Part I: Surface Roughness Effects on Heat Transfer," Acurex Corp., Aerotherm Rept. 73-80, Sept. 1973.

[24] Dirling, R.B., Jr., "Ablation/Erosion Evaluation of Reentry Vehicle Materials, Vol. I: Nosetip Materials," McDonnell Douglas Astronautics Co., AFML-TR-76-2, Feb. 1976.

[25] Deveikis, W.D. and Walker, R.W., "Local Aerodynamics Heat Transfer and Boundary-Layer Transition on Roughened Sphere-Ellipsoid Bodies at Mach Number 3.0," NASA TN D-907, 1961.

[26] Chauvin, L.T. and Spiegle, K.C., "Boundary-Layer-Transition and Heat Transfer Measurements from Flight Tests of Blunt and Sharp 50° Cones at Mach Numbers from 1.7 to 4.7," NACA RM L57004, 1957.

[27] Garland, B.J. and Chauvin, L.T., "Measurements of Heat Transfer and Boundary-Layer Transition on an 8-Inch-Diameter Hemisphere-Cylinder in Free Flight for a Mach Number Range of 2.00 to 3.88," NACA RM L57D04a, 1957.

[28] Buglia, J.J., "Heat Transfer and Boundary-Layer Transition on a Highly Polished Hemisphere Cone in Free Flight at Mach Numbers Up to 3.14 and Reynolds Numbers Up to 24×10^6," NASA TN D-955, 1961.

[29] Brick, L., "Final Report, Nosetip Design Analysis and Test Program (NDAT), Vol. I, Part I," SAMSO-TR-71-11, Oct. 1970.

[30] Dirling, R.B., Jr., "A Method for Computing Roughwall Heat Transfer Rates on Reentry Nosetips," AIAA Paper 73-763, July 1973.

[31] Dunavant, J.C. and Stone, H.W., "Effect of Roughness on Heat Transfer to Hemisphere Cylinders at Mach Numbers 10.4 and 11.4," NASA TN D-3871, 1967.

[32] Dirling, R.B., Jr., "Asymmetric Nosetip Shape Change During Atmospheric Entry," AIAA Paper 77-779, June 1977.

[33] Reda, D.C. and Leverance, R.A., "Boundary-Layer Transition Experiments on Pre-Ablated Graphite Nosetips in a Hyperballistics Range," *AIAA Journal*, Vol. 15, March 1977.

[34] Bishop, W., "Transition Induced by Distributed Roughness on Blunt Bodies in Supersonic Flow," Aerospace Corp., El Segundo, Calif., SAMSO-TR-76-146, Dec. 1976.

[35] Dyner, H.B., "Test Facilities Used for Advanced Ballistic Reentry Systems R&D," Aerospace Corp., El Segundo, Calif., Report TOR-0077 (2550-71)-2, June 20, 1977.

[36] Bishop, W., private communication, Aerospace Corp., El Segundo, Calif., 1978.

[37] Dryden, H.L., "Transition from Laminar to Turbulent Flow," *Turbulent Flows and Heat Transfer*, edited by C.C. Lin, Princeton University Press, Princeton, N.J., 1959.

[38] Wool, M.R., "Final Summary Report, Passive Nosetip Technology (PANT) Program," Aerotherm Rept. 75-159 (SAMSO-TR-75-250), June 1975.

[39] Chen, K.K. et al., "Exploratory Development of Hypersonic Heat Transfer and Thermomechanical Ablation of Advanced Materials," AVCO Systems Div., AFML-TR-75-25, April 1975.

[40] White, C.O., "Engineering Predictions for Nosetip Transition Behavior," Philco-Ford Corp., Rept. U-6118, Nov. 1974.

[41] Phinney, R.E. et al., "Influence of Roughness on Heat Transfer and Transition: ART Program Data Report," Naval Ordnance Lab., TR-73-231, Dec. 1973.

[42] van Driest, E.R. et al., "Boundary-Layer Transition on Blunt Bodies—Effect of Roughness," *AIAA Journal*, Vol. 5, Oct. 1967, pp. 1913-1915.

[43] Swigart, R.J. "Roughness-Induced Boundary-Layer Transition on Blunt Bodies," *AIAA Journal*, Vol. 10, Oct. 1972, pp. 1355-1356.

[44] Laderman, A.J., "Nosetip Transition Experimentation Program, Final Report, Vol. I," Aeronutronic Ford Corp., SAMSO-TR-76-120, June 1976.

[45] Beckwith, I.E. and Gallagher, J.J., "Heat Transfer and Recovery Temperatures on a Sphere with Laminar, Transitional, and Turbulent Boundary Layers at Mach Numbers of 2.00 and 4.15," NACA TN-4125, Dec. 1957.

[46] Bandettini, A. and Isler, W.E., "Boundary-Layer-Transition Measurements on Hemispheres of Various Surface Roughnesses in a Wind Tunnel at Mach Numbers from 2.48 to 3.55," NASA Memo 12-25-58A, March 1959.

[47] Cooper, M., Mayo, E.E., and Julius, J.D., "The Influence of Low Wall Temperature on Boundary-Layer Transition and Local Heat Transfer on 2″ Diameter Hemispheres at a Mach No. of 4.95 and a Reynolds No. per foot of 73.2×10^6," NASA TN D-391, July 1960.

[48] DiCristina, V. et al., "Laminar Surface Roughness Effects on Reentry Vehicle Nosetip Boundary Layer Transition—An Experimental Approach," ASME 75, ENAS-44, July 1975.

[49] Boudreau, A.H., Crain, W.K., and Edenfield, E.E., "Force, Pressure and Heat-Transfer Measurements on a Family of Ablated Shapes at Mach 8 and 12," Arnold Engineering Development Center, AEDC-TR-76-96, June 1976.

[50] Diaconis, N.S. et al., "Heat Transfer and Boundary-Layer Transition on Two Blunt Bodies at Mach Number 3.12," NASA TN-4099, Oct. 1957.

[51] Otis, J.H., Jr., et al., "Tast 7.5, Nosetip Ablation Phenomena, Final Report, Vol. II," AVCO Systems Div., SAMSO-TR-70-247, Nov. 1970.

[52] Holden, M.S., "Studies of Transitional Flow, Unsteady Separation Phenomena and Particle Induced Augmentation Heating on Ablated Nosetips," AFOSR-TR-76-1066, Oct. 1975.

[53] Tellup, D.M. and Denison, M.R., "X-17 Reentry Test Vehicle R-2 Final Flight Report, Part III—Analysis of Transition and Aerodynamic Heating on Nose Cone," Lockheed Missiles and Space Co., LMSC 3003.

[54] Murphy, J.D. and Rubesin, M.W., "An Evaluation of Free-Flight Test Data for Aerodynamic Heating from Laminar, Turbulent, and Transitional Boundary Layers, Part II—The X-17 Reentry Body," NASA CR 70931, April 11, 1965.

[55] Stetson, K.F. and Rushton, G.H., "Shock Tunnel Investigation of Boundary-Layer Transition at M = 5.5," *AIAA Journal*, Vol. 5, May 1967, pp. 899-906.

[56] Hall, J.R. et al., "Preliminary Results from a Free Flight Investigation of a Boundary Layer Transition and Heat Transfer on a Highly Polished 8-Inch Diameter Hemisphere Cylinder at Mach Numbers Up to 3 and Reynolds Numbers Based on a Length of 1 Foot Up to 17.7×10^6," NACA RM L57D18C, April 1957.

[57] Reda, D.C., Leverance, R.A., and Dorsey, W.G., Jr., "Application of Electro-Optical Pyrometry to Reentry Vehicle Nosetip Testing in a Hyperballistic Range," ICIASF, 1975, pp. 150-160.

[58] Reda, D.C., "Prepared Comments on Boundary-Layer Transition Research at Supersonic Velocities," Naval Surface Weapons Center, Silver Spring, Md., May 1977.

[59] Batt, R.G. and Legner, H.H., "A Review of Roughness Induced Nosetip Transition," AIAA Paper 81-1223, 1981.

[60] Liu, T.M., "Roughness Effects on a Laminar Boundary Layer and Transition," TR K210-TMK-75-1 (AVCO), Jan. 8, 1975.